NASA TECHNICAL NOTE

NASA TN D-5355

DYNAMIC STRAIN AGING IN CARBIDE STRENGTHENED MOLYBDENUM ALLOYS

by Peter L. Raffo

Lewis Research Center

Cleveland, Ohio

NATIONAL AERONAUTICS AND SPACE ADMINISTRATION • WASHINGTON, D. C. • JULY 1969

DYNAMIC STRAIN AGING IN CARBIDE STRENGTHENED MOLYBDENUM ALLOYS

By Peter L. Raffo

Lewis Research Center
Cleveland, Ohio

NATIONAL AERONAUTICS AND SPACE ADMINISTRATION

For sale by the Clearinghouse for Federal Scientific and Technical Information
Springfield, Virginia 22151 – CFSTI price $3.00

ABSTRACT

A study was made of the dynamic strain aging processes in carbide strengthened molybdenum alloys. Strengthening due to dynamic strain aging was observed in the temperature range 1500° to 2400° F (1088 to 1588 K). The strengthening is believed to arise from the pinning of mobile dislocations by metal-carbon pairs or clusters and/or carbide precipitates. This immobilization of the dislocations led to a high work-hardening rate and the observed strengthening.

DYNAMIC STRAIN AGING IN CARBIDE STRENGTHENED MOLYBDENUM ALLOYS

by Peter L. Raffo

Lewis Research Center

SUMMARY

A study was made of the dynamic strain aging processes in solution treated molybdenum-titanium-zirconium-carbon and molybdenum-zirconium-carbon alloys. Measurements of the temperature and strain rate dependence of the flow stress in solution treated alloys showed the following characteristics of dynamic strain aging: (1) a peak in the flow stress-temperature curve in the temperature range 1500° to 2400° F (1088 to 1588 K), (2) serrated stress-strain curves, (3) a negative strain-rate sensitivity in the region of the flow stress peak, and (4) a rapid rate of work hardening in the vicinity of the flow stress peak. A critical strain for the onset of serrated yielding was found that was temperature and strain-rate dependent. Observations of dislocation structure, formed during straining, showed an increased rate of dislocation multiplication with respect to strain near the flow stress peak. The flow stress was proportional to the square root of the measured dislocation density. Dynamic strain aging in molybdenum alloys is believed to arise from the immobilization of mobile dislocations by carbide precipitates or metal-carbon pairs or clusters. The pinning of the mobile dislocations leads to the increased rate of dislocation multiplication and consequently the high work-hardening rate.

INTRODUCTION

An important class of high strength molybdenum (Mo) alloys are those strengthened by the addition of a group IVA carbide former (titanium (Ti), zirconium (Zr), or hafnium (Hf)) and carbon (C). Determinations of the properties of these alloys in the wrought condition have led to the conclusion that their strength is derived from a fine dispersion of the carbides of Ti, Zr, or Hf (refs. 1 to 4).

Chang (ref. 1) and the present author (ref. 4) have measured the tensile properties

of some Mo-Ti-Zr-C and Mo-Hf-C alloys after a high temperature solution treatment. This treatment introduced a peak in the strength-temperature curve in the temperature range 1500° to 2400° F (1088 to 1588 K) accompanied by serrated plastic flow and a high work-hardening rate. In contrast, the strength of the wrought alloys decreases smoothly with increasing temperature. Chang interpreted the peak (ref. 1) as being due to the precipitation of carbides during plastic deformation, a form of dynamic strain aging. The evidence for this was mainly derived from hardness measurements made on the deformed and undeformed portions of tested tensile specimens. It was shown that age hardening occurred more rapidly in the strained portion of the tensile specimen.

The objective of the present program was to obtain data that would aid in determining a detailed mechanism of dynamic strain aging in this class of molybdenum alloys. This was accomplished by studying the temperature and strain rate dependence of the tensile stress-strain behavior of a solution treated commercial Mo-Ti-Zr-C alloy (Mo-TZC) and two experimental Mo-Zr-C alloys. The deformed alloys were also examined by transmission electron microscopy to look for the presence of strain induced carbide precipitation.

SYMBOLS

A, m, B, α	constants
b	Burgers vector
D_s	diffusion coefficient for substitutional diffusion
D_i	diffusion coefficient for interstitial diffusion
L	average distance moved by a dislocation
γ	fraction of total dislocation density which is mobile
$\dot{\epsilon}$	strain rate
ϵ_c	critical strain for the onset of serrations
μ	shear modulus
ρ	total dislocation density
ρ_m	mobile dislocation density
σ_c	critical stress for the onset of serrations
σ_f	flow stress at a strain of 0.05 min^{-1}
τ	shear flow stress

TABLE I. - DESIGNATIONS AND CHEMICAL ANALYSIS FOR MAJOR CONSTITUENTS

Designation	Composition, at. %			
	Ti	Zr	C	Mo
Mo-TZC	2.40	0.18	0.18	Bal.
Mo-ZC-1	----	.64	.49	Bal.
Mo-ZC-2	----	1.08	.74	Bal.

EXPERIMENTAL PROCEDURE

Table I lists the alloys that were studied with the chemical analysis for the major alloying elements. The Mo-TZC alloy was obtained commercially as-swaged arc-melted rod. The two Mo-Zr-C alloys were arc melted at this laboratory. The ingots were extruded at 3200° F (2033 K) and swaged at 2000° to 2500° F (1366 to 1644 K). The details of the typical melting and fabrication steps are given in another publication (ref. 4). Tensile specimens were prepared from either 0.25- or 0.13-inch (0.64- or 0.33-cm) diameter rod. The specimens had a 1-inch (2.54-cm) gage length and either a 0.16- or 0.07-inch (0.41- or 0.18-cm) gage diameter.

All specimens were initially solution annealed at 4000° F (2477 K) for 30 minutes in an induction furnace with a tungsten susceptor. The annealing was performed in a pressure of less than 10^{-5} torr. Large carbon losses (40 to 60 percent) occurred during the 4000° F (2477 K) vacuum anneal. Therefore, a small amount of molybdenum carbide (Mo_2C) powder was thus placed in the crucible with the specimens in order to minimize decarburization. Maximum losses of 10 percent were found using this technique. After heat treatment, the specimens were quenched by turning off the power and introducing helium gas into the furnace.

The specimens were electropolished at 10 to 15 volts in a 98-percent sulfuric acid electrolyte. Tensile testing was performed in a universal tensile machine at strain rates ranging from 0.002 to 2.0 reciprocal minute. Heating of the specimens below 1200° F (922 K) was accomplished using a quartz tube radiation furnace. A resistance heated tungsten mesh heater was used in the temperature range 1200° to 3000° F (922 to 1922 K). Below 1200° F (922 K), a pressure of less than 10^{-2} torr was employed; above this temperature the pressure was less than 10^{-5} torr.

Transmission electron microscopy was performed on strained tensile specimens. Slices were spark machined from the gage section at an angle of 45° to the tensile axis. The slices were then ground to thicknesses of approximately 0.25 millimeter, and a

3.2-millimeter-diameter disk was trepanned from the slice. The disks were then polished in an apparatus described by Schoone and Fishione (ref. 5). A solution of 14-percent sulfuric acid in ethanol at 30 volts and 40° to 50° F (277 to 281 K) was employed. The thinned foils were then examined in an electron microscope at 100 kilovolts.

RESULTS

The RESULTS are divided into three sections. First a section describing the temperature and strain-rate dependence of the flow stress is presented. Observations on the occurrence of serrated flow curves are presented next, followed by a final section describing the dislocation substructures generated during dynamic strain aging.

Temperature and Strain-Rate Dependence of Tensile Properties

Figure 1 shows the temperature dependence of the flow stress at a strain of 0.05 σ_f

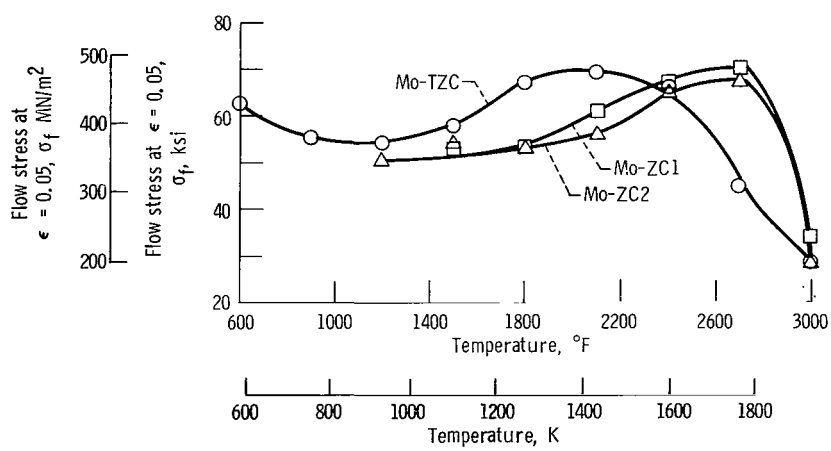

Figure 1. - Dynamic strain aging in three alloys. Materials were solution treated at 4000° F (2477 K) prior to test. Strain rate, 0.05 reciprocal minute.

for the three alloys tested. A broad flow stress maximum is seen in all the curves. The flow stress peak is sharper in the Mo-Zr-C alloys than in the Mo-TZC alloy. The peak value of σ_f occurs at approximately 2100° F (1422 K) for Mo-TZC and at approximately 2700° F (1755 K) for the two Mo-Zr-C alloys. The maximum value of σ_f is approximately 70 ksi (483 MN/m^2) for all the alloys.

The temperature dependence of σ_f for Mo-TZC was investigated over a range of

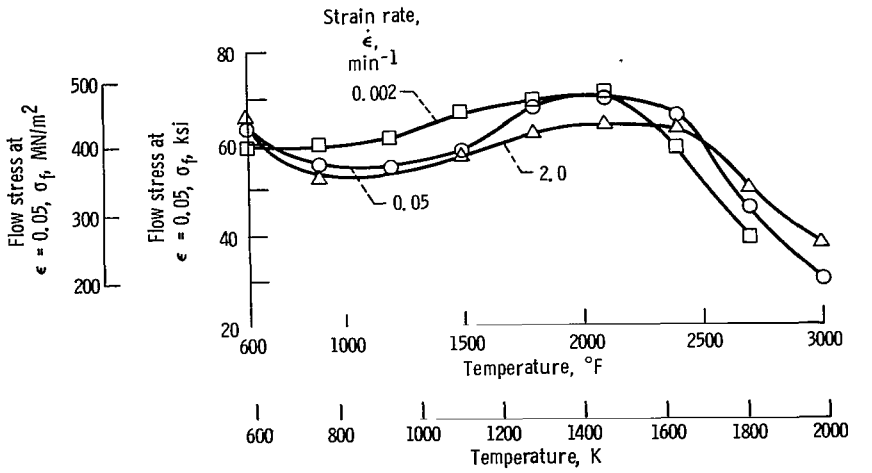

Figure 2. - Temperature and strain rate dependence of flow stress at strain of 0.05 for Mo-TZC.

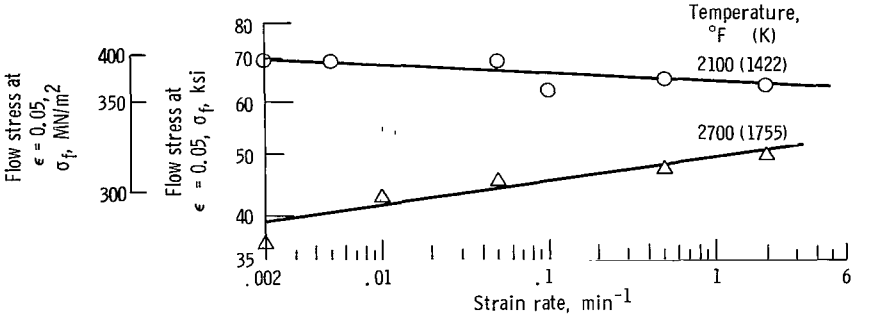

Figure 3. - Strain rate dependence of flow stress at strain of 0.05 for Mo-TZC.

strain rates from 0.002 to 2.0 reciprocal minute. Figure 2 illustrates the results at three rates. The strain-rate sensitivity of the flow stress was negative from approximately 900° F (755 K) to 2100° F (1422 K), the temperature of the flow stress peak. The maximum flow stress decreased with increasing strain rate; but the temperature for this maximum was independent of strain rate within the scale of these tests. The strain-rate sensitivity of σ_f at two temperatures is shown in more detail in figure 3. At 2100° F (1422 K) the strain-rate sensitivity is negative over the entire range of strain rates; at 2700° F (1755 K) it is positive.

Figure 4 illustrates how the level of plastic strain affects the flow stress peak. The proportional limit (stress at a strain of approximately 0.05 percent) data show a small peak at approximately 2100° F (1422 K) and the height of this peak increases with increasing plastic strain. The flow stress peak thus results from a greater rate of work hardening in the dynamic strain aging region.

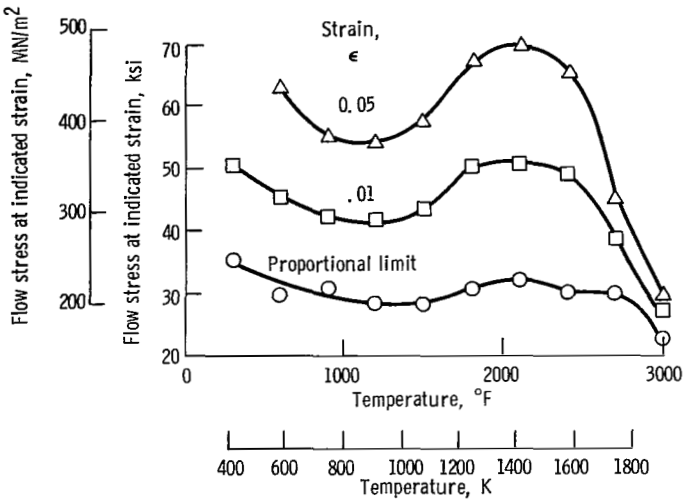

Figure 4. - Effect of temperature of flow stress at various strains for Mo-TZC. Strain rate, 0.05 reciprocal minute.

Occurrence of Serrated Flow Curves

Serrated flow curves were observed for all the alloys in a narrow range of temperatures just below the temperature of the flow stress peak. A typical serrated engineering stress-strain curve is shown in figure 5. The amplitude of the serrations was on the order of 1 ksi (7 MN/m^2) and was generally larger in the Mo-Zr-C alloys than it was in

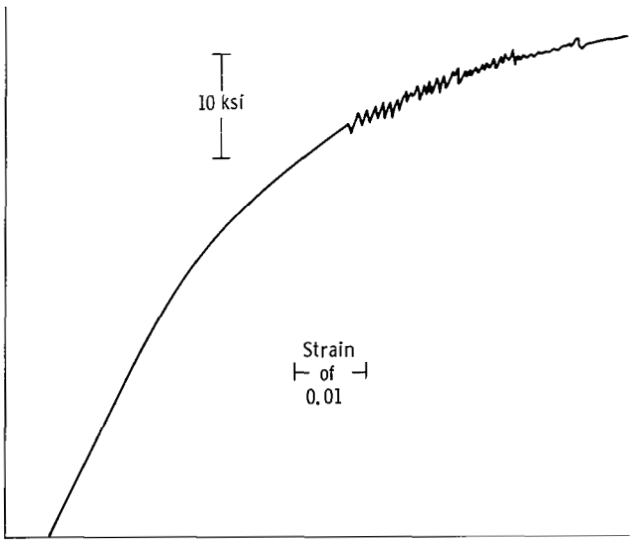

Figure 5. - Engineering stress-strain curve showing typical serrations. MZC-2 (Mo-1.08 percent Zr-0.74 percent C) tested at 1500° F; strain rate, 0.02 reciprocal minute.

the Mo-TZC. The stress-strain curves became smooth at temperatures above the flow stress peak. An attempt was made to determine an activation energy for the disappearance of the serrations by plotting the positions where serrations were observed on a $\ln \dot{\epsilon}$ versus $1/T$ plot (ref. 6). The temperature range where the serrations disappeared was so narrow that no meaningful value of the activation energy could be determined.

A characteristic of the serrated stress-strain curves for all the alloys was the existence of a critical strain ϵ_c for the onset of serrations. The existence of a critical strain is well documented for systems involving the diffusion of substitutional atoms as being rate controlling (refs. 7 to 9). The value of ϵ_c in the present work was strain-rate and temperature sensitive. Figure 6 is a plot of the strain-rate sensitivity of ϵ_c

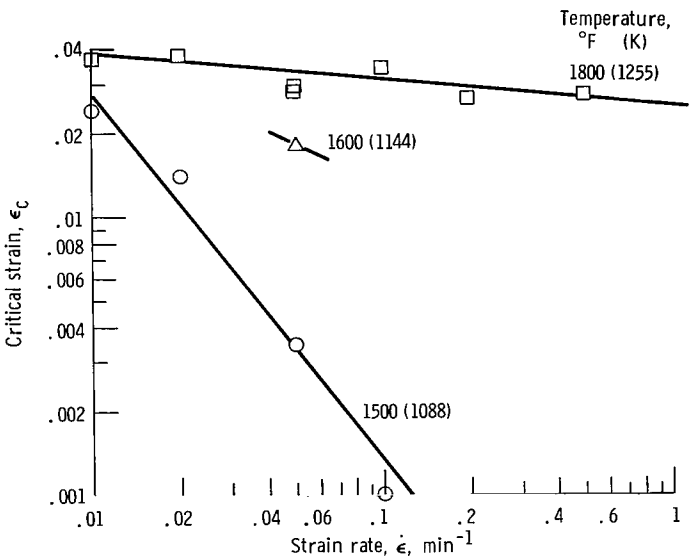

Figure 6. - Variation of critical strain with strain rate.

for MZC-2 (Mo-1.08Zr-0.74C). The value of ϵ_c could be represented by the power function

$$\epsilon_c = A\dot{\epsilon}^n \tag{1}$$

where m was -1 at 1500° F (1088 K) and -0.1 at 1800° F (1255 K). The value of ϵ_c could also be related to the stress σ_c at which the serrations began as shown in figure 7. Here a good fit was found with the relation

$$\sigma_c = \sigma_o + B\epsilon_c^{1/2} \tag{2}$$

The significance of these relations will be discussed in a later section.

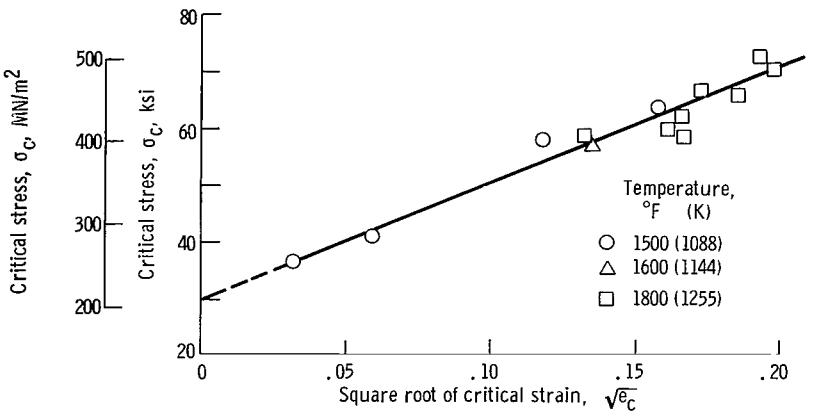

Figure 7. - Relation between critical stress and critical strain for onset of serrated yielding.

Substructure Formed During Dynamic Strain Aging of Mo-TZC

A study was made using transmission electron microscopy of the substructure formed during straining. The study was conducted entirely on specimens of Mo-TZC. Table II gives the conditions under which the specimens were strained and the relevant data that were obtained.

TABLE II. - TENSILE AND DISLOCATION DENSITY DATA FOR Mo-TZC, INITIAL SOLUTION TREATMENT AT 4000° F (2477 K)

Specimen	Test temperature		Strain rate, min^{-1}	Strain, ϵ	Flow stress, σ		Dislocation density, ρ, cm^{-2}	Rate of dislocation multiplication, $k_\rho = \rho/\epsilon$, cm^{-2}
	°F	K			ksi	MN/m^2		
1	1200	922	0.010	0.051	57.00	393	40.8×10^8	8.0×10^{10}
2	1800	1255	.002	.066	63.90	434	67.5	10.2
3	2100	1422	.010	.056	68.80	474	62.5	11.2
4	2100	1422	2.00	.090	67.80	468	68.1	7.6
5	2700	1755	.01	.042	41.30	285	44.4	10.6
6	2750	1783	.10	.227	52.70	363	42.2	1.9
7	3000	1922	.01	.044	24.6	177	6.6	1.5

Figure 8. - Mo-TZC solution treated condition prior to testing. Note apparent dislocation generation near molybdenum carbide platelet A.

Figure 8 is a micrograph of Mo-TZC in the as-solution-treated condition. As has been shown previously (refs. 1 and 10), complete suppression of precipitation during cooling is virtually impossible in this alloy. The platelets that are seen in figure 8 are apparently Mo_2C, which precipitated during the quench. The dislocation density is low, and these dislocations may have been generated by thermal stresses around the carbides during the quench (see A in the micrograph).

The micrographs that will now be described were made from specimens strained at 0.01 reciprocal minute at 1200°, 2100°, 2700°, and 3000° F (922, 1422, 1755, and 1922 K). These temperatures were chosen to encompass the flow stress peak for Mo-TZC observed in figure 1. The dislocation structures were similar at 1200° and 2100° F (922 and 1422 K) being characterized by considerable tangling around the Mo_2C platelets (figs. 9 and 10). Isolated examples of precipitation on dislocations was observed. However, if the effect were more general, the precipitates were too small to be resolved.

Dislocation structures formed at 2700° and 3000° F (1755 and 1922 K) are shown in figures 11 and 12. The dislocation density is lower than at lower temperatures and precipitation has advanced further. Figure 11 shows a large number of fine (approx 100 Å or 10 nm) particles alined in arrays suggesting nucleation on dislocations. The possibility exists that these particles were also present on the dislocations at 2100° F (1422 K)

Figure 9. - Mo-TZC strained 0.051 at 1200° F (922 K) at a strain rate of 0.01 reciprocal minute. Foil plane, $(\bar{1}10)$; operating reflections, $[\bar{1}\bar{1}2]$ and [110]. X45 000

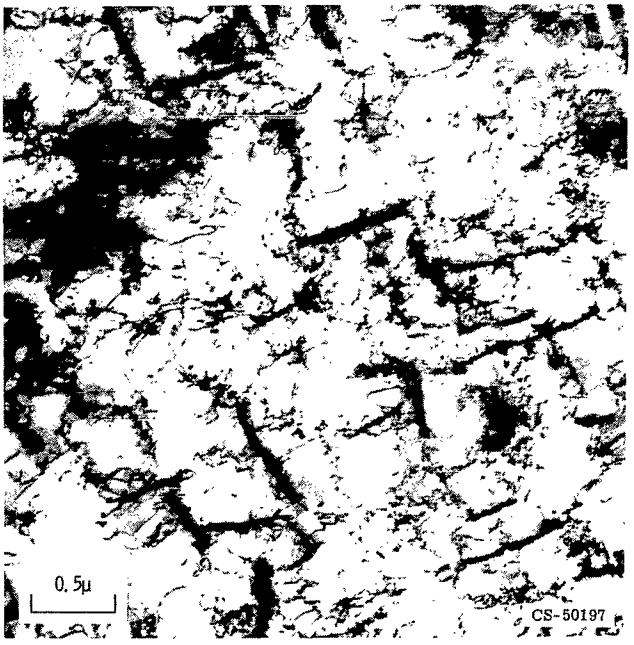

Figure 10. - Mo-TZC strained 0.056 at 2100° F (1422 K) at strain rate of 0.01 reciprocal minute. Foil plane, (301); operating reflection, [020]. X40 000

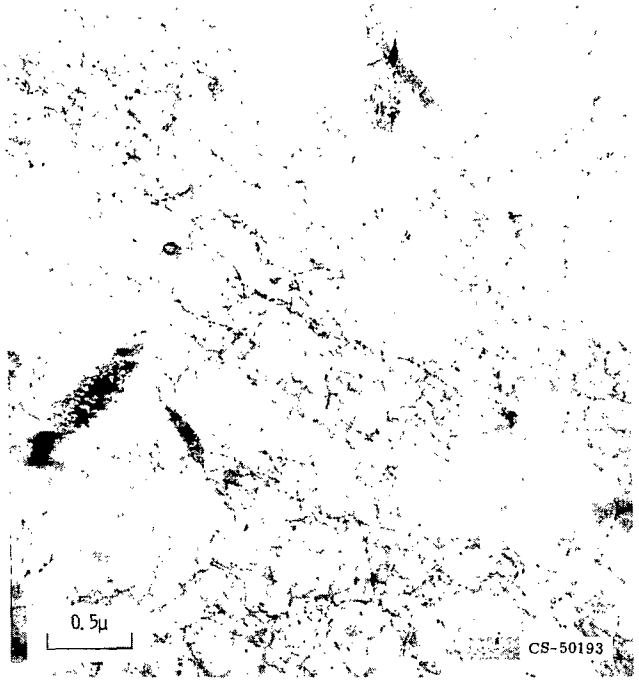

Figure 11. - Mo-TZC strained 0.042 at 2700° F (1755 K) at strain rate of 0.01 reciprocal minute. Foil plane, (111); multiple operating reflections. X45 000

Figure 12. - Mo-TZC strained 0.044 at 3000° F (1922 K) at strain rate of 0.01 reciprocal minute. Foil plane, (111); operating reflections, $[\bar{2}11]$, $[10\bar{1}]$. X45 000

but could not be resolved. After deformation at 3000° F (1922 K), precipitation has proceeded further and the dislocation density is quite low. The Mo_2C platelets have apparently been replaced by general precipitation of a (Ti, Zr) C face centered cubic carbide, as has been observed previously by other investigators (refs. 1 and 10). Some of this precipitation took place on dislocations, while some of it took place in the matrix. The dual nucleation site for (Ti, Zr) C is in agreement with the results of Ryan and Martin (ref. 10) on a similar alloy.

Table I gives the dislocation density ρ measured on these and other samples. The value of ρ was measured using the technique of Ham (ref. 11). In one of the columns a rate of dislocation multiplication was calculated by assuming that the dislocation density-strain relation was linear (ref. 12). It is apparent that the value of K_d passes through a maximum at the same temperature where the maximum flow stress was observed. Figure 13 is a plot of the flow stress in these alloys versus the square root of the measured

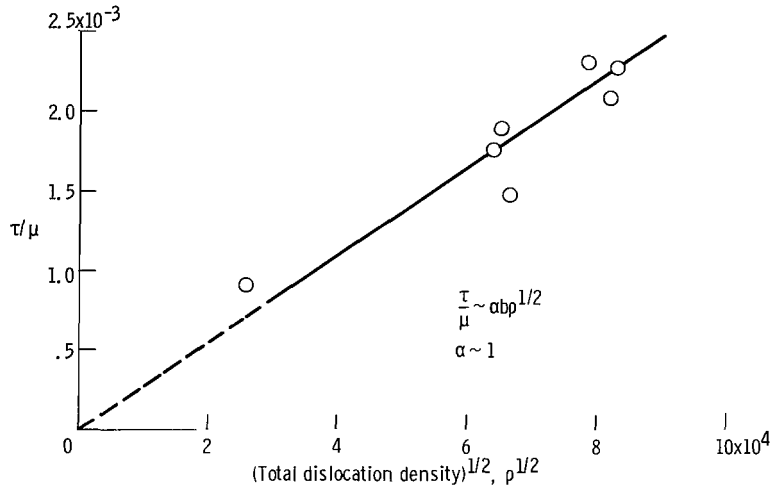

Figure 13. - Relation between flow stress and dislocation density.

dislocation density. It is apparent that the high flow stress in the dynamic strain aging region is directly associated with a high dislocation density by the relation:

$$\frac{\tau}{\mu} = \alpha b \rho^{1/2} \tag{3}$$

where τ is the shear flow stress (taken as half the tensile flow stress), μ is the shear modulus at temperature (values taken from Armstrong and Brown, ref. 13), b is the Burger's vector, and α is a dimensionless constant which is nearly unity. Thus, the substructural studies bear out the results in figure 4 that the strengthening during dy-

namic strain aging is a work-hardening effect brought about by an increased rate of dislocation multiplication. The association of a high work hardening with dynamic strain aging has been observed previously in steels (refs. 7 and 14) and vanadium (ref. 15).

DISCUSSION

In the preceding sections the characteristics of dynamic strain aging in three molybdenum base alloys have been described. It was shown that the peak in the flow stress-temperature curve in the temperature range 2100° to 2700° F (1422 to 1755 K) was caused by an increased work-hardening rate resulting from an increased rate of dislocation multiplication. The instantaneous flow stress and dislocation density could be related to one another as shown in figure 13.

The fact that an increased work-hardening rate results from dynamic strain aging in other body centered cubic metals and alloys is well documented in the literature (ref. 7). This behavior may be rationalized by assuming that dislocations are immobilized in some way during deformation, thus reducing the mobile dislocation density. For example, in a constant strain-rate tensile test, the product of the dislocation velocity and the mobile dislocation density must remain constant. Fresh mobile dislocations must be produced to replace those that have become immobilized, which leads to the high rate of dislocation multiplication.

The question still remains as to what atomic specie or precipitate in the present alloys is responsible for the immobilization. This will be the subject of the remainder of the discussion.

Immobilization Mechanisms

In the molybdenum alloys studied in this work the characteristics of dynamic strain aging are observed over a wide temperature range extending from approximately 700° to 2100° F (544 to 1422 K). This is particularly noticeable in the extent of the negative strain-rate sensitivity of Mo-TZC shown in figure 2. It was shown previously (ref. 7) that, when dynamic strain aging in body centered cubic metals results from the diffusion of interstitial atoms or the precipitation of a matrix atom-interstitial compound, the effects are maximized when

$$\frac{\dot{\epsilon}}{D_i} = 10^9 \tag{4}$$

where $\dot{\epsilon}$ is the strain rate and D_i is the diffusion coefficient of the relevant interstitial.

If values of D_i for carbon in molybdenum (ref. 17) are substituted into equation (4), dynamic strain aging should occur in the temperature range of approximately 850° to 1100° F (727 to 866 K). These temperatures are at the lower end of the range where dynamic strain aging is observed for the present alloys. Brock (ref. 16) noted that dynamic strain aging occurs very weakly in nominally unalloyed molybdenum. He attributed this to the low solubility of interstitials in molybdenum. It is thus doubtful whether single interstitials are contributing much in the present alloys as well.

The fact that dynamic strain aging in these alloys extends to much higher temperatures suggests that the diffusion of slower moving specie such as a substitutional atom contributes to the observed effects. It is not clear, however, whether the strengthening arises from the diffusion of substitutional atoms behind moving dislocations producing a drag stress (ref. 18) or from their actual precipitation as a second phase. The observation made of a critical strain ϵ_c for the onset of serrated flow could be helpful here. A critical strain for serrated flow is a characteristic of dynamic strain aging in alloys where vacancy migration is necessary for diffusion. This is a consequence of a relation between the strain rate and diffusion coefficient similar to equation (4). The value of D_s, the coefficient for substitutional diffusion, is strain dependent, however, since vacancies can be created during deformation. The strain at which the concentration of vacancies and consequently the value of D_s reaches a critical value is thus the critical strain ϵ_c.

The strain rate and temperature dependence of the critical strain in the present alloys is opposite to that which is usually observed (refs. 8 and 9). Generally, the critical strain is smaller at higher temperatures and lower strain rates where fewer vacancies must be created during straining in order to reach the critical diffusion coefficient. This anomalous behavior suggests that the diffusion of substitutional atoms is not solely responsible for dynamic strain aging on these alloys. This conclusion was also reached by Mukherjee et al. (ref. 9) who observed similar anomalies in the critical strain behavior at high temperatures in an aluminum alloy.

Dynamic strain aging in these molybdenum base alloys may then result from actual precipitation on dislocations. In the present work, extensive precipitation of carbides was observed only at 2700° and 3000° F (1755 and 1922 K) above the temperature where the maximum strain aging effects were observed. However, the possibility of unresolvable precipitates at the lower straining temperatures should not be disregarded. Ryan and Martin (ref. 10) have made extensive observations of carbide precipitation in alloys similar to those studied here. They found that precipitation begins with the formation of small, coherent platelets on {001} or {310} planes (depending on the specific carbide). Their lowest aging temperature was 2192° F (1573 K). There thus exists the possibility of forming an even simpler metal-carbon configuration below this temperature. These configurations could be simple Ti (or Zr)-C pairs or clusters. Roy et al. (ref. 19) have

claimed Mossbauer spectroscopy evidence for this type of configuration in Fe-Mn-N alloys where the strengthening effects are similar to those found in the present molybdenum alloys (ref. 20).

The Critical Strain for Onset of Serrated Flow

If carbide precipitation on dislocations controlled the strengthening of the molybdenum alloys, then the critical strain for the onset of serrated flow may arise from some event other than strain induced vacancy formation. One such event may be deduced from consideration of equation (2), which related the critical stress σ_c to the critical strain ϵ_c:

$$\sigma_c = \sigma_o + B\epsilon_c^{1/2}$$

The critical strain may be expressed in terms of the mobile dislocation density ρ_m and the average distance that dislocations move L by

$$\epsilon_c = \rho_m bL \tag{5}$$

If we assume that ρ_m is the same fraction γ of the total dislocation density ρ, then substitution of equation (5) into equation (2) gives

$$\sigma_c = \sigma_o + B(bL\gamma)^{1/2}\rho^{1/2} \tag{6}$$

This relation between the flow stress and the dislocation density was observed in figure 13 for the Mo-TZC alloy. Since the slope of the $\sigma_c - \epsilon_c^{1/2}$ curve was constant, it implies that the value of L may be the critical factor controlling the onset of serrations.

CONCLUDING REMARKS

A study has been made of dynamic strain aging in three carbide strengthened molybdenum alloys. It appears likely that the increase in the flow stress during dynamic strain aging is a work-hardening effect brought about by an increased rate of dislocation multiplication. However, the specie responsible for the immobilization of dislocations

during straining is obscure. The question of whether an actual precipitate or a simpler metal-carbon cluster causes the immobilization may have to be resolved by other experimental techniques.

Lewis Research Center,
National Aeronautics and Space Administration,
Cleveland, Ohio, June 2, 1969,
129-03-02-08-22.

REFERENCES

1. Chang, W. H.: Effect of Heat Treatment on Strength Properties of Molybdenum Base Alloys. Trans. ASM, vol. 56, 1963, pp. 107-124.

2. Chang, W. H.: Effect of Carbide Dispersion in Molybdenum Alloys. Trans. AIME, vol. 218, no. 2, Apr. 1960, pp. 254-256.

3. Chang, W. H.: Strain-Induced vs. Pre-Existing Precipitation in the Mo-TZC Alloy. Trans. ASM, vol. 57, 1964, pp. 565-567.

4. Raffo, Peter L.: Exploratory Study of Mechanical Properties and Heat Treatment of Molybdenum-Hafnium-Carbon Alloys. NASA TN D-5025, 1969.

5. Schoone, R. D.; and Fischione, E. A.: Automatic Unit for Thinning Transmission Electron Microscopy Specimens of Metals. Rev. Sci. Instr., vol. 37, no. 10, Oct. 1966, pp. 1351-1353.

6. Keh, A. S.; Nakada, Y.; and Leslie, W. C.: Dynamic Strain Aging in Iron and Steel. Dislocation Dynamics. McGraw-Hill Book Co., Inc., 1968, pp. 381-407.

7. Klein, M. J.; and Reid, C. N.: Strain Aging. Metal Deformation Processing, Vol. 1. DMIC Rep. 208, Battelle Memorial Inst., Aug. 14, 1964, pp. 114-126. (Available from DDC as AD-608637).

8. Charnock, W.: The Influence of Grain Size on the Nature of Portevin-Lechatelier Yielding. Phil. Mag., vol. 18, no. 151, July 1968, pp. 89-99.

9. Mukherjee, K.; D'Antonio, C.; Maciag, R.; and Fischer, G.: Impurity-Dislocation Interaction and Repeated Yielding in a Commercial Al Alloy. J. Appl. Phys., vol. 39, no. 12, Nov. 1968, pp. 5434-5440.

10. Ryan, N. E.; and Martin, J. W.: Hardening of Molybdenum-Base Alloys by Precipitation of Nitride and Carbide Phases. Presented at the Plansee Metallwerke Seminar, Reulette, -Tyrol, Austria, June 1968.

11. Ham, R. K.: The Determination of Dislocation Densities in Thin Films. Phil. Mag., vol. 6, no. 69, Sept. 1961, pp. 1183-1184.

12. Johnston, W. G.; and Gilman, J. J.: Dislocation Velocities, Dislocation Densities, and Plastic Flow in Lithium Fluoride Crystals. J. Appl. Phys., vol. 30, no. 2, Feb. 1959, pp. 129-144.

13. Armstrong, Philip E.; and Brown, Harry L.: Dynamic Young's Modulus Measurements Above 1000° C on Some Pure Polycrystalline Metals and Commercial Graphites. Trans. AIME, vol. 230, no. 5, Aug. 1964, pp. 962-966.

14. Baird, J. D.; and MacKenzie, C. R.: Effects of Nitrogen and Manganese on the Deformation Substructure of Iron Strained at 20°, 225°, and 450° C. J. Iron Steel Inst., vol. 202, pt. 5, May 1964, pp. 427-436.

15. Edington, J. W.; and Smallman, R. E.: The Relationship Between Flow Stress and Dislocation Density in Deformed Vanadium. Acta Met., vol. 12, no. 12, Dec. 1964, pp. 1313-1328.

16. Brock, G. W.: Strain Aging Effects in Arc-cast Molybdenum. Trans. AIME, vol. 221, no. 5, Oct. 1961, pp. 1055-1062.

17. Rudman, P. S.: The Solubility Limit and Diffusivity of Carbon in Molybdenum. Trans. AIME, vol. 239, no. 12, Dec. 1967, pp. 1949-1954.

18. Cottrell, A. H.: Interactions of Dislocations and Solute Atoms. Relation of Properties to Microstructure. ASM, 1954, pp. 131-162.

19. Roy, Ram B.; Solly, B.; and Wäppling, R.: An Investigation of the High Temperature Strengthening Mechanism in a Dilute Fe-Mn-N Alloy by Means of the Mössbauer Effect. Zeit. f. Metallk., vol. 59, no. 7, July 1968, pp. 563-566.

20. Baird, J. D.; and Jamieson, A.: The Effects of Carbon, Nitrogen and Manganese on the High-Temperature Tensile Properties of Iron. Relation Between the Structure and Mechanical Properties of Metals. Nat. Phys. Lab. Gt. Brit., Symp., vol. 15, no. 1, 1963, pp. 362-377.

NATIONAL AERONAUTICS AND SPACE ADMINISTRATION
WASHINGTON, D. C. 20546
OFFICIAL BUSINESS

FIRST CLASS MAIL

POSTAGE AND FEES PAID
NATIONAL AERONAUTICS AND
SPACE ADMINISTRATION

POSTMASTER: If Undeliverable (Section 158 Postal Manual) Do Not Return

"The aeronautical and space activities of the United States shall be conducted so as to contribute . . . to the expansion of human knowledge of phenomena in the atmosphere and space. The Administration shall provide for the widest practicable and appropriate dissemination of information concerning its activities and the results thereof."

—NATIONAL AERONAUTICS AND SPACE ACT OF 1958

NASA SCIENTIFIC AND TECHNICAL PUBLICATIONS

TECHNICAL REPORTS: Scientific and technical information considered important, complete, and a lasting contribution to existing knowledge.

TECHNICAL NOTES: Information less broad in scope but nevertheless of importance as a contribution to existing knowledge.

TECHNICAL MEMORANDUMS: Information receiving limited distribution because of preliminary data, security classification, or other reasons.

CONTRACTOR REPORTS: Scientific and technical information generated under a NASA contract or grant and considered an important contribution to existing knowledge.

TECHNICAL TRANSLATIONS: Information published in a foreign language considered to merit NASA distribution in English.

SPECIAL PUBLICATIONS: Information derived from or of value to NASA activities. Publications include conference proceedings, monographs, data compilations, handbooks, sourcebooks, and special bibliographies.

TECHNOLOGY UTILIZATION PUBLICATIONS: Information on technology used by NASA that may be of particular interest in commercial and other non-aerospace applications. Publications include Tech Briefs, Technology Utilization Reports and Notes, and Technology Surveys.

Details on the availability of these publications may be obtained from:

SCIENTIFIC AND TECHNICAL INFORMATION DIVISION

NATIONAL AERONAUTICS AND SPACE ADMINISTRATION

Washington, D.C. 20546